Energy Shaping for Vehicles with Point Mass Actuators

C. Konda Reddy and Craig A. Woolsey

***Abstract*— This paper describes the application of the method of controlled Lagrangians to vehicles with moving point mass actuators. This class of systems includes certain spacecraft, atmospheric re-entry vehicles, and underwater vehicles. Two examples are presented. The first example is a spinning disk, a simplified, planar version of a spacecraft spin stabilization problem. The second example is an underwater vehicle moving in the horizontal plane.**

I. INTRODUCTION

Moving mass actuators (MMAs) occupy a small but important niche among vehicle actuators. Because they can be housed inside a vehicle's chassis, MMAs are protected from the surrounding environment. And because their effectiveness relies on action/reaction or on gravity rather than on relative fluid motion, these actuators can be used in environments or operating conditions where conventional actuators may be ineffective. Internal MMAs are used to control maneuverable atmospheric re-entry vehicles, for example, because they are protected from the high temperatures and forces that arise in hypersonic flight [13], [7]. MMAs have also been proposed for precision orbit control in spacecraft formations [15]; passive versions have long been used on spacecraft as nutation dampers. MMAs are also useful for controlling buoyancy-driven underwater gliders, a new class of long-endurance autonomous underwater vehicle (AUV). In this application, because they are protected from corrosion and biological fouling, MMAs remain reliable actuators for deployments of months or even years [5], [9], [16], [17].

Control design using MMAs is challenging because multibody dynamic models are relatively high-dimensional. Lyapunov-based control design methods are appealing for such high-dimensional systems. Moreover, these methods can provide stability and control results that hold over a larger domain than can be obtained using linear design and analysis. The principal objective of this paper is to illustrate the application of an energy-based control design technique, the method of controlled Lagrangians, for stabilizing steady vehicle motions using moving mass actuators. We anticipate that this approach may ultimately be used to develop nonlinear controllers for complex vehicle control problems such as maneuverable re-entry vehicles.

Section II describes a dynamic model for a vehicle with a finite number of MMAs. Section III reviews the method of controlled Lagrangians. Section IV describes a simple example of a spinning disk with a MMA. Section V presents a slightly more complicated example, a streamlined underwater vehicle in planar motion. As the example illustrates, however, deriving a feedback control law which shapes the closed-loop energy does not necessarily ensure computable conditions for stability. In this example, the control-modified energy fails to provide satisfiable conditions for stability. This does not mean that the control law fails to stabilize the system; spectral analysis provides simple conditions for local stability. It does mean, however, that the analysis falls short of the original objective. Constructing Lyapunov functions is a fundamental challenge which energy shaping methods can only begin to address.

II. VEHICLE DYNAMIC MODEL

Figure 1 depicts a rigid body, immersed in an infinite volume of ideal fluid that is at rest at infinity, along with n point masses. In general, the body may apply control forces to these point masses, thus coupling the elements of the system. For now, we assume that the point masses are free to move in three dimensions. In examples, we will consider the case of one MMA which is confined to a linear track. For a detailed discussion of dynamic modeling for vehicles with point mass actuators, see [18]. The control objective is to stabilize steady rotations of the rigid body by applying control forces to the point masses. The control design problem is especially challenging because the system is underactuated.

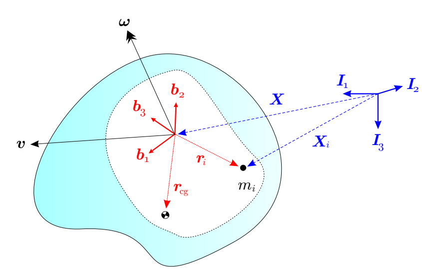

Fig. 1. A rigid body in an ideal fluid with n internal moving masses.

Let $m_{\rm rb}$ be the mass of the rigid body and let m_i be the mass of the $i^{\rm th}$ point mass. We assume that the system is neutrally buoyant; that is, we assume that $m = m_{\rm rb} + \sum_{i=1}^{n} m_i$ is equal to the mass of fluid displaced by the rigid body. Let $\boldsymbol{I}_1$, $\boldsymbol{I}_2$, and $\boldsymbol{I}_3$ be an orthonormal triad defining an inertial reference frame and let $\boldsymbol{b}_1$, $\boldsymbol{b}_2$, and $\boldsymbol{b}_3$ be another orthonormal triad representing a reference frame fixed at some point in the rigid body. The body frame rotates with angular velocity $\boldsymbol{\omega}$ and translates with velocity $\boldsymbol{v}$ with respect to the inertial frame, where both vectors are expressed in the

C. Konda Reddy is a post-doc at the Nonlinear Systems Lab (NSL), Aerospace and Ocean Engineering, Virginia Tech, Blacksburg, VA 24061, USA konda@vt.edu

Craig Woolsey is with the faculty of Aerospace and Ocean Engineering, Virginia Tech, Blacksburg, VA 24061, USA cwoolsey@vt.edu

body frame. Similarly, the i^{th} point mass moves with velocity $\boldsymbol{v}_i$ with respect to inertial space. (Throughout the paper, lower case boldfaced characters represent vectors expressed in the body frame. Upper case boldfaced vectors represent vectors expressed in the inertial frame. Exceptions will be clear from context.)

If $\boldsymbol{R}$ represents the proper rotation matrix which transforms free vectors from the body to the inertial frame, then the system kinematics are

$$\begin{aligned}\dot{\boldsymbol{R}} &= \boldsymbol{R}\hat{\boldsymbol{\omega}}\\ \dot{\boldsymbol{X}} &= \boldsymbol{R}\boldsymbol{v}\\ \dot{\boldsymbol{X}}_1 &= \boldsymbol{R}\boldsymbol{v}_1\\ &\vdots\\ \dot{\boldsymbol{X}}_n &= \boldsymbol{R}\boldsymbol{v}_n\end{aligned}$$

where $\hat{\boldsymbol{a}}$ denotes the skew symmetric matrix satisfying $\hat{\boldsymbol{a}}\boldsymbol{b} = \boldsymbol{a}\times\boldsymbol{b}$ for vectors $\boldsymbol{a},\boldsymbol{b}\in\Re^3$.

Because the system is immersed in an ideal fluid, the body's motion induces motion in the surrounding fluid (and vice versa). The effect is captured by the *added mass* and *added inertia*, which account for the additional energy that is necessary to accelerate the fluid around the body as it moves. If the rigid body has uniformly distributed mass and three planes of symmetry, and if the body frame is chosen appropriately, then the combined body/fluid inertia and mass matrices $\boldsymbol{I}_{\mathrm{b/f}}$ and $\boldsymbol{M}_{\mathrm{b/f}}$ are diagonal.

The examples given in Sections IV and V involve planar systems for which the effect of gravity vanishes. Although it is straightforward to include forces and moments due to gravity in the dynamic model (see [18], for example), our model ignores gravity in the interest of brevity. Let $\boldsymbol{h}$ and $\boldsymbol{p}$ represent the angular momentum and translational momentum, respectively, of the complete body/fluid/point mass system about the body frame origin. Strictly speaking, $\boldsymbol{h}$ and $\boldsymbol{p}$ are the impulse required to effect the body translational velocity $\boldsymbol{v}$ and angular velocity $\boldsymbol{\omega}$ (as well as the resulting motion of the fluid). As shown in [8], the time evolution of these quantities is described by a finite set of ordinary differential equations which resemble the momentum equations for a rigid body moving in a vacuum. Let $\boldsymbol{p}_i$ represent the translational momentum of the i^{th} point mass. Suppose that the body applies a force $\boldsymbol{u}_i$ to the i^{th} point mass. Then the dynamic equations can be obtained using Newton's laws as

$$\begin{aligned}\dot{\boldsymbol{h}} &= \boldsymbol{h}\times\boldsymbol{\omega} + \boldsymbol{p}\times\boldsymbol{v}\\ \dot{\boldsymbol{p}} &= \boldsymbol{p}\times\boldsymbol{\omega}\\ \dot{\boldsymbol{p}}_1 &= \boldsymbol{p}_1\times\boldsymbol{\omega} + \boldsymbol{u}_1\\ &\vdots\\ \dot{\boldsymbol{p}}_n &= \boldsymbol{p}_n\times\boldsymbol{\omega} + \boldsymbol{u}_n. \end{aligned}\tag{1}$$

Let

$$\boldsymbol{\eta} = \begin{pmatrix}\boldsymbol{\omega}\\ \boldsymbol{v}\end{pmatrix} \quad \text{and} \quad \boldsymbol{r} = \begin{pmatrix}\boldsymbol{r}_1\\ \vdots\\ \boldsymbol{r}_n\end{pmatrix},$$

where $\boldsymbol{r}_i$ is the location of the i^{th} point mass relative to the body frame origin. The term $\boldsymbol{\eta}$ appears as a vector of generalized velocities, although its components are not time derivatives of any well-defined generalized coordinates. The kinetic energy for this system is

$$l(\boldsymbol{\eta},\boldsymbol{r},\dot{\boldsymbol{r}}) = \frac{1}{2}\begin{pmatrix}\boldsymbol{\eta}\\ \dot{\boldsymbol{r}}\end{pmatrix}^T \boldsymbol{M}(\boldsymbol{r})\begin{pmatrix}\boldsymbol{\eta}\\ \dot{\boldsymbol{r}}\end{pmatrix}\tag{2}$$

where the matrix components of the kinetic energy metric

$$\boldsymbol{M} = \begin{pmatrix}\boldsymbol{M}_1 & \boldsymbol{M}_4 & \boldsymbol{M}_5\\ \boldsymbol{M}_4^T & \boldsymbol{M}_2 & \boldsymbol{M}_6\\ \boldsymbol{M}_5^T & \boldsymbol{M}_6^T & \boldsymbol{M}_3\end{pmatrix}$$

are

$$\begin{aligned}\boldsymbol{M}_1 &= \boldsymbol{I}_{\mathrm{b/f}} - \sum_{i=1}^{n} m_i\hat{\boldsymbol{r}}_i\hat{\boldsymbol{r}}_i\\ \boldsymbol{M}_2 &= \boldsymbol{M}_{\mathrm{b/f}} + \left(\sum_{i=1}^{n} m_i\right)\boldsymbol{\mathcal{I}}\\ \boldsymbol{M}_3 &= \mathrm{diag}(m_1\boldsymbol{\mathcal{I}},\ldots,m_n\boldsymbol{\mathcal{I}})\\ \boldsymbol{M}_4 &= \sum_{i=1}^{n} m_i\hat{\boldsymbol{r}}_i\\ \boldsymbol{M}_5 &= [m_1\hat{\boldsymbol{r}}_1 \quad \ldots \quad m_n\hat{\boldsymbol{r}}_n]\\ \boldsymbol{M}_6 &= [m_1\boldsymbol{\mathcal{I}} \quad \ldots \quad m_n\boldsymbol{\mathcal{I}}].\end{aligned}$$

(In the expressions above, $\boldsymbol{\mathcal{I}}$ represents the 3×3 identity matrix.) We note that

$$\boldsymbol{h} = \frac{\partial l}{\partial \boldsymbol{\omega}}, \quad \boldsymbol{p} = \frac{\partial l}{\partial \boldsymbol{v}}, \quad \text{and} \quad \boldsymbol{p}_i = \frac{\partial l}{\partial \dot{\boldsymbol{r}}_i}.$$

The dynamics (1) can be rewritten as

$$\begin{pmatrix}\frac{d}{dt}\frac{\partial l}{\partial \boldsymbol{\eta}}\\ \frac{d}{dt}\frac{\partial l}{\partial \dot{\boldsymbol{r}}} - \frac{\partial l}{\partial \boldsymbol{r}}\end{pmatrix} = \begin{pmatrix}\boldsymbol{\Lambda} & \boldsymbol{0}\\ \boldsymbol{0} & \boldsymbol{0}\end{pmatrix}\begin{pmatrix}\boldsymbol{\eta}\\ \dot{\boldsymbol{r}}\end{pmatrix} + \begin{pmatrix}\boldsymbol{0}\\ \boldsymbol{\mathcal{I}}\end{pmatrix}\boldsymbol{u}.\tag{3}$$

In (3), the matrix $\boldsymbol{\Lambda}$ is a skew-symmetric matrix whose components depend on the components of $\frac{\partial l}{\partial \boldsymbol{\eta}}$. The matrix $\boldsymbol{\mathcal{I}}$ is an identity matrix of appropriate dimensions.

For the examples considered in this paper, there is only one moving point mass which is constrained to move along a linear track. It is a simple matter to adapt the model above to this case. For example, suppose that the linear track is parallel to the body $\boldsymbol{b}_1$-axis. One simply requires that $\dot{\boldsymbol{r}}_1\cdot\boldsymbol{e}_2 = 0$ and $\dot{\boldsymbol{r}}_1\cdot\boldsymbol{e}_3 = 0$, where $\boldsymbol{e}_i$ is the i^{th} basis vector for $\Re^3$; see [18].

III. The Method of Controlled Lagrangians

In this section, we review the method of controlled Lagrangians in the notation of [19]. This method is a nonlinear stabilization technique for underactuated mechanical systems. Formally introduced in [3], the technique was refined and expanded in a series of follow-on papers. Put simply, the method provides a feedback control law under which the closed-loop dynamics of a given Lagrangian system derive from a new, control-modified Lagrangian. In its most general setting, the method involves kinetic and potential energy shaping and allows for generalized gyroscopic forces in the closed-loop equations; see [4], [14], [19]. The idea of kinetic energy shaping has enjoyed a great deal of attention in recent years, in both the Lagrangian and Hamiltonian settings. In addition to the series of papers beginning with [3], relevant papers in the Lagrangian setting include [1] and [6] and references therein. On the Hamiltonian side, see [2] or [12], for example, and references therein.

To begin the review, assume that the Euler-Lagrange equations hold for a mechanical system with Lagrangian

$$L(\boldsymbol{q}, \dot{\boldsymbol{q}}) = \frac{1}{2}\dot{\boldsymbol{q}}^T \boldsymbol{M}(\boldsymbol{q})\dot{\boldsymbol{q}} - V(\boldsymbol{q}) \qquad (4)$$

where $\boldsymbol{M}(\boldsymbol{q})$ is the positive definite kinetic energy metric, $V(\boldsymbol{q})$ is the potential energy, and $\boldsymbol{q} = \begin{bmatrix}\boldsymbol{q}_{\mathrm{u}}^T & \boldsymbol{q}_{\mathrm{a}}^T\end{bmatrix}^T$ is the vector of generalized coordinates. Coordinates $\boldsymbol{q}_{\mathrm{u}}$ are unactuated; coordinates $\boldsymbol{q}_{\mathrm{a}}$ are actuated. Here, we do not assume any symmetry in the system. Symmetries, if present, can be used to reduce the dimension of the dynamics. Ignoring dissipation, the Euler-Lagrange equations may be rewritten in the form

$$\boldsymbol{M}(\boldsymbol{q})\ddot{\boldsymbol{q}} + \boldsymbol{C}(\boldsymbol{q}, \dot{\boldsymbol{q}})\dot{\boldsymbol{q}} + \frac{\partial V}{\partial \boldsymbol{q}} = \begin{pmatrix}\boldsymbol{0}\\ \boldsymbol{u}\end{pmatrix}, \qquad (5)$$

where $\boldsymbol{C}$ is the standard "Coriolis and centripetal" matrix associated with $\boldsymbol{M}$ [11]. The input $\boldsymbol{u}$ has the dimension of $\boldsymbol{q}_{\mathrm{a}}$.

If successfully applied, the method of controlled Lagrangians provides a control law and a modified Lagrangian $L_c(\boldsymbol{q}, \dot{\boldsymbol{q}})$ for which the closed-loop equations become

$$\boldsymbol{M}_c(\boldsymbol{q})\ddot{\boldsymbol{q}} + \boldsymbol{C}_c(\boldsymbol{q}, \dot{\boldsymbol{q}})\dot{\boldsymbol{q}} + \frac{\partial V_c}{\partial \boldsymbol{q}} = \boldsymbol{\mathcal{S}}_c(\boldsymbol{q}, \dot{\boldsymbol{q}})\dot{\boldsymbol{q}} \qquad (6)$$

where $\boldsymbol{M}_c$ is a control-modified kinetic energy metric, V_c is a control-modified potential energy, and $\boldsymbol{\mathcal{S}}_c(\boldsymbol{q}, \dot{\boldsymbol{q}})$ is skew-symmetric. The conditions under which such a control law exists are called the "matching conditions." Skew-symmetry of $\boldsymbol{\mathcal{S}}_c$ ensures that the control-modified energy corresponding to L_c is conserved. The generalized force $\boldsymbol{\mathcal{S}}_c(\boldsymbol{q}, \dot{\boldsymbol{q}})\dot{\boldsymbol{q}}$ is referred to as "gyroscopic" in analogy with a class of uncontrolled physical systems with similar dynamics [4].

The matching conditions are derived by comparing equations (5) and (6) and then choosing the control $\boldsymbol{u}$ and the free parameters in L_c so that (6) holds. Solving (6) for $\ddot{\boldsymbol{q}}$ and substituting into the open-loop equations (5) relates the original system parameters $\boldsymbol{M}$ and V to the control-modified parameters $\boldsymbol{M}_c$, V_c, and $\boldsymbol{\mathcal{S}}_c$ [19]:

$$\begin{pmatrix}\boldsymbol{0}\\ \boldsymbol{u}\end{pmatrix} = \boldsymbol{M}\boldsymbol{M}_c^{-1}\left[\boldsymbol{\mathcal{S}}_c\dot{\boldsymbol{q}} - \boldsymbol{C}_c\dot{\boldsymbol{q}} - \frac{\partial V_c}{\partial \boldsymbol{q}}\right] + \boldsymbol{C}\dot{\boldsymbol{q}} + \frac{\partial V}{\partial \boldsymbol{q}} \qquad (7)$$

The matching conditions are given by the first n equations in (7), where n is the dimension of $\boldsymbol{q}_{\mathrm{u}}$. The matching conditions are a set of non-linear PDEs in $\boldsymbol{M}_c$ and V_c with $\boldsymbol{\mathcal{S}}_c$ free to choose. Solving the matching conditions for $\boldsymbol{M}_c$, V_c and $\boldsymbol{\mathcal{S}}_c$, (7) gives the control input $\boldsymbol{u}$. Having obtained a control-modified Lagrangian system, one may study closed-loop stability of equilibria by treating the control-modified total energy

$$E_c(\boldsymbol{q}, \dot{\boldsymbol{q}}) = \frac{1}{2}\dot{\boldsymbol{q}}^T \boldsymbol{M}_c(\boldsymbol{q})\dot{\boldsymbol{q}} + V_c(\boldsymbol{q})$$

as a control Lyapunov function. Having found control parameters such that a given equilibrium is a minimum (or a maximum) of E_c, one may apply feedback dissipation to make $\dot{E}_c \le 0$ (or $\dot{E}_c \ge 0$). One may then assess asymptotic stability using LaSalle's principle.

The method of controlled Lagrangians can be applied to vehicles with MMAs exactly as it applies to classical Lagrangian systems by recognizing that

$$\begin{pmatrix}\frac{d}{dt}\frac{\partial l}{\partial \boldsymbol{\eta}}\\ \frac{d}{dt}\frac{\partial l}{\partial \dot{\boldsymbol{r}}} - \frac{\partial l}{\partial \boldsymbol{r}}\end{pmatrix} = \boldsymbol{M}(\boldsymbol{q})\ddot{\boldsymbol{q}} + \boldsymbol{C}(\boldsymbol{q}, \dot{\boldsymbol{q}})\dot{\boldsymbol{q}} \qquad (8)$$

where $\boldsymbol{q}^T = [\boldsymbol{\Theta}^T, \boldsymbol{r}^T]$ and where $\dot{\boldsymbol{\Theta}} = \boldsymbol{\eta}$. Note that $\boldsymbol{\Theta}$ is not a meaningful coordinate, but a quasi-coordinate. Thus, $\boldsymbol{M}$ does not depend on $\boldsymbol{\Theta}$. Though the quasi-coordinate does not have a physical meaning, its introduction helps us to put the equations in the traditional controlled Lagrangian framework. One may proceed with the method of controlled Lagrangians exactly as before, with the understanding that the control-modified kinetic metric must also not depend on $\boldsymbol{\Theta}$.

We assume that there is no actuation in the quasi-coordinate directions and the internal dynamics are fully actuated. Thus, we let $\boldsymbol{q}_{\mathrm{u}} = \boldsymbol{\Theta}$ and $\boldsymbol{q}_{\mathrm{a}} = \boldsymbol{r}$. Referring to equations (3) and (8),

$$\boldsymbol{M}(\boldsymbol{q})\ddot{\boldsymbol{q}} + \boldsymbol{C}(\boldsymbol{q}, \dot{\boldsymbol{q}})\dot{\boldsymbol{q}} = \boldsymbol{\mathcal{S}}(\boldsymbol{q}, \dot{\boldsymbol{q}})\dot{\boldsymbol{q}} + \boldsymbol{G}\boldsymbol{u},$$

where

$$\boldsymbol{\mathcal{S}} = \begin{pmatrix}\boldsymbol{\Lambda} & \boldsymbol{0}\\ \boldsymbol{0} & \boldsymbol{0}\end{pmatrix} \quad \text{and} \quad \boldsymbol{G} = \begin{pmatrix}\boldsymbol{0}\\ \boldsymbol{\mathcal{I}}\end{pmatrix}.$$

Note that all entries of $\boldsymbol{M}$, $\boldsymbol{C}$ and $\boldsymbol{\mathcal{S}}$ are independent of $\boldsymbol{q}_{\mathrm{u}}$. Applying the method of controlled Lagrangians gives

$$\boldsymbol{M}_c(\boldsymbol{q})\ddot{\boldsymbol{q}} + \boldsymbol{C}_c(\boldsymbol{q}, \dot{\boldsymbol{q}})\dot{\boldsymbol{q}} = \boldsymbol{\mathcal{S}}_c(\boldsymbol{q}, \dot{\boldsymbol{q}})\dot{\boldsymbol{q}}.$$

Comparing the open- and closed-loop equations above gives

$$\boldsymbol{\mathcal{S}}_c\dot{\boldsymbol{q}} = \boldsymbol{M}_c\boldsymbol{M}^{-1}(\boldsymbol{G}\boldsymbol{u} + \boldsymbol{\mathcal{S}}\dot{\boldsymbol{q}} - \boldsymbol{C}\dot{\boldsymbol{q}}) + \boldsymbol{C}_c\dot{\boldsymbol{q}}. \qquad (9)$$

Let the components of $\boldsymbol{u}$ be quadratic in velocity:

$$u^i(\boldsymbol{q}, \dot{\boldsymbol{q}}) = u^i_{jk}(\boldsymbol{q})\dot{q}^j\dot{q}^k.$$

Then we may write

$$\boldsymbol{G}\boldsymbol{u} = \boldsymbol{U}(\boldsymbol{q}, \dot{\boldsymbol{q}})\dot{\boldsymbol{q}},$$

where the non-zero components of the matrix $\boldsymbol{U}$ are linear in velocity. Equation (9) becomes,

$$\boldsymbol{\mathcal{S}}_c\dot{\boldsymbol{q}} = (\boldsymbol{M}_c\boldsymbol{M}^{-1}(\boldsymbol{U} + \boldsymbol{\mathcal{S}} - \boldsymbol{C}) + \boldsymbol{C}_c)\dot{\boldsymbol{q}}.$$

Skew-symmetry of $\boldsymbol{\mathcal{S}}_c$ gives

$$\dot{\boldsymbol{q}}^T(\boldsymbol{M}_c\boldsymbol{M}^{-1}(\boldsymbol{U} + \boldsymbol{\mathcal{S}} - \boldsymbol{C}) + \boldsymbol{C}_c)\dot{\boldsymbol{q}} = 0. \qquad (10)$$

The scalar equation (10) is cubic in velocity. Restricting the closed-loop dynamics to be unconstrained, we may collect coefficients of like terms and set each to zero. Eliminating the control components u^i_{jk} from these equations gives the matching conditions. Having satisfied these conditions, one may solve for the control law.

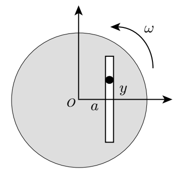

Fig. 2. A spinning disk with a point mass moving along a slot

Nonlinear stability analysis for this type of system involves not only the control-modified energy but also any other quantities that may be conserved under the system motion. These additional conserved quantities are typically associated with inertial momentum conservation laws. The energy-Casimir method described in [10] provides one constructive approach for proving Lyapunov stability.

IV. Example: A Spinning Disk

In this section, we illustrate the controlled Lagrangian technique for a simple example. Consider a planar disk spinning about its center O as shown in Figure 2. A point mass m moves, under the influence of a control force, along a linear track in the disk which is displaced some distance $a \neq 0$ from the center. Let I be the moment of inertia of the disk about its spin axis.

Define the non-dimensional quantities

$$\bar{y} = \frac{y}{a}; \quad \bar{\omega} = \frac{\omega}{\omega_0}; \quad \tau = \omega_0 t \quad \text{and} \quad \alpha = \frac{I}{ma^2} + 1,$$

where $\omega_0 \neq 0$ is some reference angular rate. Dropping the bar for convenience, the non-dimensional Lagrangian is

$$l = \frac{1}{2} \begin{pmatrix} \omega \\ \dot{y} \end{pmatrix}^T \begin{pmatrix} \alpha + y^2 & 1 \\ 1 & 1 \end{pmatrix} \begin{pmatrix} \omega \\ \dot{y} \end{pmatrix}.$$

In the absence of physical dissipation, the equations of motion are

$$\begin{aligned} \frac{d}{dt}\left(\frac{\partial l}{\partial \omega}\right) &= 0 \\ \frac{d}{dt}\left(\frac{\partial l}{\partial \dot{y}}\right) - \frac{\partial l}{\partial y} &= u, \end{aligned} \tag{11}$$

where u is the control applied to the point mass. The eigenvalues corresponding to the relative equilibrium $(\omega, y, \dot{y}) = (1, 0, 0)$ are $\lambda_1 = 0$ and $\lambda_{2,3} = \pm\sqrt{\alpha/(\alpha-1)}$. Since $\alpha > 1$, the equilibrium is a saddle point. The zero eigenvalue corresponds to conservation of total angular momentum $\frac{\partial l}{\partial \omega}$.

We seek an energy shaping control u_{es} such that the closed-loop equations are Lagrangian. Following Section III, we obtain a matching solution for which

$$\boldsymbol{M}_c = \begin{pmatrix} \alpha + y^2 & 1 \\ 1 & \frac{\beta}{\alpha + y^2} \end{pmatrix} \quad \text{and} \quad \boldsymbol{\mathcal{S}}_c = \mathbf{0},$$

where $\beta \neq 1$ is a control parameter. A family of matching control laws for systems with one unactuated degree of freedom is reported in [1]. The above matching law leads to a closed-loop kinetic energy metric that has a simple structure. The kinetic energy shaping control is

$$\begin{aligned} u_{\text{es}} = & \frac{(\alpha + y^2 - \beta) y \omega^2}{(\beta - 1)} + \\ & \frac{2(\alpha + y^2)(\alpha + y^2 - \beta)\omega y \dot{y} + \beta(\alpha + y^2 - 1) y \dot{y}^2}{(\beta - 1)(\alpha + y^2)^2}. \end{aligned}$$

Next, we prove nonlinear stability of the equilibrium using the energy-Casimir method [10]. The total angular momentum $C = (\alpha + y^2)\omega + \dot{y}$ is a Casimir.

Proposition 4.1: The energy shaping control u_{es} stabilizes the relative equilibrium $(\omega, y, \dot{y}) = (1, 0, 0)$ provided $\beta < 1$.

Proof: The control modified energy E_c and C are conserved quantities. Let $E_\phi = E_c + \phi(C)$ be a candidate Lyapunov function, where $\phi(\cdot)$ is an as-yet-undetermined smooth function. Nonlinear stability of the equilibrium will follow from Lyapunov's direct method if

$$\nabla E_\phi\big|_e = 0 \quad \text{and} \quad \nabla^2 \, E_\phi\big|_e > 0 \text{ (or} < 0),$$

where ∇E_ϕ and $\nabla^2 E_\phi$ denote the gradient and Hessian of E_ϕ respectively. Upon calculation,

$$\nabla E_\phi\big|_e = \begin{pmatrix} \alpha \left(\frac{\partial \phi}{\partial C}\Big|_e + 1 \right) \\ 0 \\ \frac{\partial \phi}{\partial C}\Big|_e + 1 \end{pmatrix}$$

and

$$\nabla^2 E_\phi\big|_e = \begin{pmatrix} \alpha + \alpha^2 \frac{\partial^2 \phi}{\partial C^2}\Big|_e & 0 & 1 + \alpha \frac{\partial^2 \phi}{\partial C^2}\Big|_e \\ 0 & 1 + 2 \frac{\partial \phi}{\partial C}\Big|_e & 0 \\ 1 + \alpha \frac{\partial^2 \phi}{\partial C^2}\Big|_e & 0 & \frac{\partial^2 \phi}{\partial C^2}\Big|_e + \frac{\beta}{\alpha} \end{pmatrix}.$$

The equilibrium can be made a maximum of E_ϕ by choosing

$$\frac{\partial \phi}{\partial C}\Big|_e = -1; \quad \frac{\partial^2 \phi}{\partial C^2}\Big|_e < -\frac{1}{\alpha} \quad \text{and} \quad \beta < 1.$$

A choice for ϕ is $\phi(C) = \frac{\delta}{2} C^2 - (1 + \delta\alpha) C$ where $\delta < -\frac{1}{\alpha}$. ■

Feedback dissipation can now be used make the equilibrium asymptotically stable. When dissipation is added, E_c is no longer conserved, though C is still conserved. In this case, $\dot{E}_\phi = \dot{E}_c$. Let

$$u_{\text{diss}} = \frac{k_{\text{diss}} \dot{y} (\alpha + y^2 - 1)}{\beta - 1}.$$

Choosing $k_{\text{diss}} > 0$ makes $\dot{E}_c \geq 0$ and thus $\dot{E}_\phi \geq 0$. Asymptotic stability follows from LaSalle's invariance principle.

V. Example: A Planar AUV

In this section, we consider the problem of stabilizing steady, long-axis translation of a streamlined underwater vehicle using a single MMA mounted orthogonally to the desired axis of translation. We restrict our attention to the planar case. While the example may seem academic, it is relevant to the problem of directional stabilization for rudderless underwater gliders. These vehicles use moving

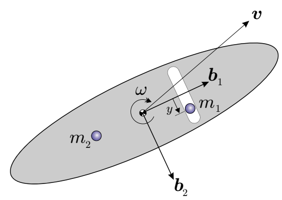

Fig. 3. A planar underwater vehicle with two point masses. One mass is fixed and the other moves along a track under the influence of a control force u.

mass actuators for attitude control because external actuators, such as control planes and thrusters, can easily foul or corrode. The problem is also reminiscent of re-entry vehicle stabilization as described in [7].

Figure 3 depicts an elliptical planar underwater vehicle with a single MMA. The vehicle moves with translational velocity $\boldsymbol{v} = [v_1,\ v_2]^T$ and angular velocity ω. An actuated mass m_1 moves along a track which is parallel to the body $\boldsymbol{b}_2$-axis and offset some distance a forward of the geometric center, $\boldsymbol{r}_1 = (a, y(t))$. (In this analysis, it makes no difference whether the mass is forward or aft of the geometric center.) To simplify analysis, another point mass $m_2 = m_1$ is fixed at the location $\boldsymbol{r}_2 = (-a, 0)$.

We use a, m and a/v_o for length, mass and time scaling, respectively, where v_o is some desired steady translational speed. The nondimensional inertia is I, the nondimensional mass in the $\boldsymbol{b}_1$ direction is M_1, and the nondimensional mass in the $\boldsymbol{b}_2$ direction is M_2. We let l_i represent the length of the vehicle along the $\boldsymbol{b}_i$ axis. Assuming that $l_1 > l_2$, it follows that $M_2 > M_1$. Moreover, we have $I > 2$ and $M_{1,2} > 2$.

Let $r = y$ and let $\boldsymbol{\eta} = (\omega,\ v_1,\ v_2)^T$. Then the Lagrangian is given by (2), where

$$\boldsymbol{M} = \begin{pmatrix} I + y^2 & -y & 0 & 1 \\ -y & M_1 & 0 & 0 \\ 0 & 0 & M_2 & 1 \\ 1 & 0 & 1 & 1 \end{pmatrix}.$$

The nondimensional equations of motion are given by (3) where

$$\boldsymbol{\Lambda} = \begin{pmatrix} 0 & -\frac{\partial l}{\partial v_2} & \frac{\partial l}{\partial v_1} \\ \frac{\partial l}{\partial v_2} & 0 & 0 \\ -\frac{\partial l}{\partial v_1} & 0 & 0 \end{pmatrix}.$$

The square of the momentum magnitude $P_s = (\frac{\partial l}{\partial v_1})^2 + (\frac{\partial l}{\partial v_2})^2$ is conserved and the dynamics evolve on a surface of constant P_s. The equilibrium of interest is

$$(\omega,\ v_1,\ v_2,\ y,\ \dot{y}) = (0,\ 1,\ 0,\ 0,\ 0). \qquad (12)$$

Because the system is Hamiltonian (see [18]), the eigenvalues of the linearized dynamics are distributed symmetrically about the real and imaginary axes. One of the eigenvalues is zero, reflecting conservation of total linear momentum. The remaining four eigenvalues either appear in pure real conjugate pairs, pure imaginary conjugate pairs, or as a complex conjugate quartet. For spectral stability, all eigenvalues must be located on the imaginary axis. For the uncontrolled system, the eigenvalues corresponding to the equilibrium are

$$\lambda_{1,2,3} = 0 \text{ and } \lambda_{4,5} = \pm\sqrt{\frac{(M_2 - M_1)(M_1 - 1)}{I(M_2 - 1) - M_2}}.$$

We have

$$I(M_2 - 1) - M_2 = IM_2 \left[1 - \left(\frac{1}{I} + \frac{1}{M_2}\right)\right].$$

Since $I, M_2 > 2$, it follows that $I(M_2 - 1) - M_2 > 0$. Because $\lambda_{4,5}$ constitutes a real conjugate pair, the equilibrium is a saddle. The two additional zero eigenvalues reflect the degenerate nature of the equilibrium; any state of the form $(\omega,\ v_1,\ v_2,\ y,\ \dot{y})^T = (0, 1, 0, \tilde{y}, 0)^T$ is an equilibrium.

Following the procedure outlined in Section III, we find a matching control law such that

$$\boldsymbol{M}_c = \begin{pmatrix} I + y^2 & -y & 0 & 1 \\ -y & M_1 & 0 & 0 \\ 0 & 0 & M_2 & 1 \\ 1 & 0 & 1 & \rho \end{pmatrix} \quad \text{and} \quad \boldsymbol{\mathcal{S}}_c = \boldsymbol{\mathcal{S}}.$$

In order to make the equilibrium an isolated equilibrium, we introduce an artificial potential function $V_c = \frac{1}{2}ky^2$. The control parameters are thus ρ and k. We observed that the above choice of a matching law does not lead to a proof of nonlinear stability. In lieu of a proof of nonlinear stability, we determine values of k and ρ for spectral stability.

Proposition 5.1: There exist values of k and ρ for which (12) is spectrally stable.

Proof: Each eigenvalue λ for the closed loop system satisfies

$$\lambda(\lambda^4 + \frac{\mu_1}{\mu_3}\lambda^2 + \frac{\mu_2}{\mu_3}) = 0 \qquad (13)$$

where

$$\begin{aligned} \mu_1 &= -kIM_2 + (\rho M_1 - 1)(M_2 - M_1) \\ \mu_2 &= kM_1(M_2 - M_1);\ \mu_3 = I + (1 - \rho I)M_2. \end{aligned}$$

As noted earlier, the zero eigenvalue corresponds to conservation of total linear momentum. For spectral stability, the remaining eigenvalues must lie on the imaginary axis. This will occur only if

$$\frac{\mu_1}{\mu_3} > 0, \quad \frac{\mu_2}{\mu_3} > 0, \quad \text{and} \quad \mu_1^2 - 4\mu_2\mu_3 > 0. \qquad (14)$$

Let us assume $I < \frac{M_1 M_2}{M_2 - M_1}$. A similar proof follows when $I > \frac{M_1 M_2}{M_2 - M_1}$. The curve $\phi(k, \rho) = \mu_1^2 - 4\mu_2\mu_3 = 0$ passes through the intersection of $\mu_1 = 0$ and $\mu_3 = 0$ and the intersection of $\mu_1 = 0$ and $\mu_2 = 0$. The lines $\mu_1 = 0$, $\mu_2 = 0$, and $\mu_3 = 0$ are shown schematically in Figure 4 (a), where

$$\rho_1 = \frac{1}{M_1} \quad \text{and} \quad \rho_2 = \frac{I + M_2}{IM_2} > \frac{1}{M_1}.$$

Note that the curve $\phi(k, \rho) = 0$ is quadratic in k and ρ. When $k = 0$, $\phi(0, \rho) = (M_2 - M_1)^2(1 - M_1\rho)^2$. Thus $\phi(0, \rho) = 0$ has a double root at $\rho = 1/M_1$. This implies that the ρ axis is tangent to the curve $\phi = 0$ at $\rho = 1/M_1$.

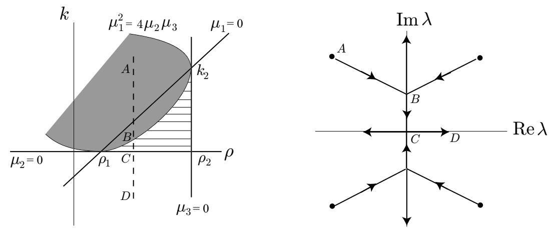

(a) (b)

Fig. 4. (a) Linear stability boundaries in the $(k,\ \rho)$ space. (b) Eigenvalue movement as k is decreased.

Similarly, the line $\mu_3 = 0$ is tangent to the curve at (ρ_2, k_2). Since $\phi = 0$ is quadratic, the above observations suggest that the curve $\phi = 0$ has the form as shown schematically in Figure 4 (a). Also, $\phi(0, 0) = (M_2 - M_1)^2 > 0$. Thus, $\phi > 0$ outside the shaded region in 4 (a). The triangle formed by $\mu_1 = 0,\ \mu_2 = 0$ and $\mu_3 = 0$ represents the region where $\frac{\mu_1}{\mu_3} > 0$ and $\frac{\mu_2}{\mu_3} > 0$. Thus, the hashed region represents the parameter values of k and ρ for which the spectral stability conditions in (14) are satisfied. ■

The movement of the eigenvalues as k is varied is shown schematically in Figure 4 (b). At point A, as shown in 4 (a), there exists a symmetric quartet of eigenvalues. As k is decreased, the eigenvalues move towards the imaginary axis. At point B, $\phi = 0$ and the system undergoes a Hamiltonian Hopf bifurcation. From B to C, the eigenvalues move along the imaginary axis. One pair moves towards the origin and coalesces at C ($k = 0$). As k is decreased further, this pair splits apart, moving in opposite directions along the real axis.

Corollary 5.2: The equilibrium cannot be stabilized using potential shaping alone.

Proof: Note that $\rho = 1$ corresponds to the case where there is no kinetic shaping. The proof follows from the observation that $1 > \rho_2 = \frac{1}{I} + \frac{1}{M_2}$ as $I > 2$ and $M_2 > 2$. Thus, the line $\rho = 1$ lies outside the stability region shown in Figure 4 (a). ■

VI. Conclusions

The method of controlled Lagrangians is a promising nonlinear stabilization method for vehicles with internal actuators. The control technique was applied to vehicle systems with moving mass actuators. Examples of this class of systems include underwater gliders and re-entry vehicles. We have studied two systems to illustrate the idea. For the spinning disk example, an asymptotically stabilizing energy shaping controller was derived. For the planar underwater example, the control modified energy failed to satisfy conditions for nonlinear stability. However, the control law is locally stabilizing and there exist control parameter values for which the desired equilibrium is spectrally stable. The example illustrates that deriving a energy shaping control law does not necessarily guarantee nonlinear stability and warrants further research in the application of energy shaping control to real engineering problems. Though the examples considered in this paper are simple examples, we anticipate that this control technique can be applied to complex control vehicle problems.

References

[1] D. Auckly and L. Kapitanski. Control of nonlinear underactuated systems. *JCO Journal on Control and Optimization*, 41(5):1372–1388, 2002.

[2] G. Blankenstein, R. Ortega, and A. van der Schaft. The matching conditions of controlled Lagrangians and IDA-passivity based control. *International Journal of Control*, 75(9):645–665, 2000.

[3] A. M. Bloch, N. E. Leonard, and J. E. Marsden. Stabilization of mechanical systems using controlled Lagrangians. In *Proceedings of the IEEE Conference on Decision and Control*, pages 2356–2361, 1997.

[4] D. E. Chang, A. M. Bloch, N. E. Leonard, J. E. Marsden, and C. A. Woolsey. The equivalence of controlled Lagrangian and controlled Hamiltonian systems for simple mechanical systems. *ESAIM: Control, Optimisation, and Calculus of Variations*, 8:393–422, 2002. Special issue dedicated to J.L. Lions.

[5] C. C. Eriksen, T. J. Osse, R. D. Light, T. Wen, T. W. Lehman, P. L. Sabin, J. W. Ballard, and A. M. Chiodi. Seaglider: A long-range autonomous underwater vehicle for oceanographic research. *Journal of Oceanic Engineering*, 26(4):424–436, 2001. Special Issue on Autonomous Ocean-Sampling Networks.

[6] J. Hamberg. General matching conditions in thetheory of controlled lagrangians. In *Proceedings of the IEEE Conference on Decision and Control*, pages 2519–2523, 1999.

[7] R. D. Robinett III, B. R. Sturgis, and S. A. Kerr. Moving-mass trim control for aerospace vehicles. *AIAA Journal of Guidance, Control, and Dynamics*, 19(5):1064–1070, 1996.

[8] H. Lamb. *Hydrodynamics*. Dover, New York, NY, sixth edition, 1932.

[9] N. E. Leonard and J. G. Graver. Model-based feedback control of autonomous underwater gliders. *Journal of Oceanic Engineering*, 26(4):633–645, 2001. Special Issue on Autonomous Ocean-Sampling Networks.

[10] J. E. Marsden and T. S. Ratiu. *Introduction to Mechanics and Symmetry*. Springer-Verlag, 1994.

[11] R. M. Murray, Z. Li, and S. S. Sastry. *A Mathematical Introduction to Robotic Manipulation*. CRC Press, 1994, Ann Arbor, MI.

[12] R. Ortega, M. W. Spong, F. Gómez-Estern, and G. Blankenstein. Stabilization of a class of underactuated mechanical systems via interconnection and damping assignment. *IEEE Transactions on Automatic Control*, 47(8):1218–1233, 2002.

[13] T. Petsopoulos, F. J. Regan, and J. Barlow. Moving-mass roll control system for fixed-trim re-entry vehicle. *Journal of Spacecraft and Rockets*, 33(1):54–60, 1996.

[14] C. K. Reddy. *Practical challenges in the method of controlled Lagrangians*. PhD thesis, Virginia Tech, 2005.

[15] I. M. Ross. Mechanism for precision orbit control with applications to formation flying. *AIAA Journal of Guidance, Control, and Dynamics*, 25(4):818–820, 2002.

[16] J. Sherman, R. E. Davis, W. B. Owens, and J. Valdes. The autonomous underwater glider “Spray”. *Journal of Oceanic Engineering*, 26(4):437–446, 2001. Special Issue on Autonomous Ocean-Sampling Networks.

[17] D. C. Webb, P. J. Simonetti, and C. P. Jones. SLOCUM: An underwater glider propelled by environmental energy. *Journal of Oceanic Engineering*, 26(4):447–452, 2001. Special Issue on Autonomous Ocean-Sampling Networks.

[18] C. A. Woolsey. Reduced Hamiltonian dynamics for a rigid body coupled to a moving mass particle. *AIAA Journal of Guidance, Control, and Dynamics*, 28(1):131–138, 2005.

[19] C. A. Woolsey, C. K. Reddy, A. M. Bloch, D. E. Chang, N. E. Leonard, and J. E. Marsden. General matching in the method of controlled Lagrangians. *European Journal of Control (Special Issue on Lagrangian and Hamiltonian Methods for Nonlinear Control)*, 10(5):478–496, 2004.